Hierarchical Structure in Polymeric Materials

E. BAER, A. HILTNER, H. D. KEITH

The diversity of monomers available for synthesis of high polymers makes it possible to prepare a wide variety of long-chain macromolecular compounds. It is instructive to consider a hierarchical organization of structure in polymers at four successive levels—the molecular, nano-, micro-, and macrolevels—and to examine how interactions at and between these various levels of structure have important and often quite specific influences. Examples are drawn from semicrystalline polymers with flexible chains, liquid-crystalline polymers composed of rigid macromolecules, and amorphous polymers. Structural hierarchies in biocomposite systems are also discussed, particularly in soft connective tissues such as tendon and intervertebral disk.

THE DEVELOPMENT AND APPLICATION OF SOPHISTICATED polymeric systems has been a major technological advance. Polymers are used in plastics, composites, textiles, packaging, coatings, adhesives, and rubbers. These materials have high-technology applications that demand the realization and control of highly specific properties. These properties can include high mechanical strength, rigidity, toughness, the ability to perform adequately under extreme environmental conditions, electrical conductivity, and piezoelectrical response. In this article, we focus on the concept of the hierarchical structure as a basis for the design and control of polymer properties. Some of the challenges in applying this understanding to the development of new materials and the need for corresponding advances in processing techniques have recently been outlined by Bement (*1*). He has emphasized the value and appropriateness of considering structure in such materials on four levels, namely, the molecular, nano-, micro-, and macroscales. We discuss factors that govern structure in polymers and illustrate particular hierarchies in examples drawn from amorphous and semicrystalline synthetic polymers and from natural biological polymers of specific structure and function.

The primary structure of the macromolecule, in terms of the sequence and number of monomers, stereoregularity, and molecular weight, can be manipulated by polymer synthesis. Commercial polymers are designed to control chain stiffness and the nature of intra- and intermolecular interactions. As greater complexity is imparted, either by side group or main chain modification, more structure is built into the macromolecule, so that the resulting polymer has more sophisticated properties. This is evident in biological systems, where genetic coding produces precise sequences in proteins. Although advanced polymers are obviously made without the complex coding of the biological macromolecule, a large variety of structures can be synthesized. Table 1 shows a representative sampling of polymer structures and corresponding transition temperatures (*2*). Amorphous polymers have a glass transition temperature but no melting temperature. They are stiff below that temperature and highly viscous above it. Semicrystalline polymers have both a melting temperature and a glass transition temperature, the latter referring to the amorphous regions that surround crystallites.

A remarkable breakthrough was the discovery about 30 years ago of novel heterogeneous catalysts for stereospecific polymerization. These catalysts allowed the control of stereochemical configuration such that the pendant side groups were placed in a regular manner along the main chain. Polymers that were previously known only in amorphous form could now be produced as isomers that readily crystallized. More recently, macromolecules with stiff chains have been synthesized with aromatic groups in the main chain. Such polymers have outstanding strength at high temperatures. Rigid aromatic polymers can also exhibit liquid-crystalline behavior. This imparts flow-induced alignment of the molecules during processing that is reflected in high degrees of orientation in the resulting solid-state structure.

The synthesis of block polymers is another important development. A well-known example has molecules that consist of a length or block of styrene homopolymer (a polymer with only one type of monomer unit) covalently bonded to a block of butadiene homopolymer. This is a diblock polymer. Triblock polymers consist of two components, one of which is sandwiched between the other two. Multiple block polymers are also known. An important property of these block polymers is controlled phase separation, which leads to enhanced impact resistance.

Modified Amorphous Polymers

The so-called atactic or amorphous polymers cannot crystallize because side groups adopt random configurations. Therefore, they are used at temperatures below their glass transition temperature. Materials such as polystyrene and polymethyl methacrylate are examples of typical polymeric glasses that are quite brittle unless a second toughening component is added. A typical problem with such materials is crazing or cracking. Upon deformation, this type of glass crazes prior to catastrophic fracture. The crazes are oriented perpendicular to the direction of the applied stress; in Fig. 1, a craze in polystyrene is shown (*3*). A single craze is reinforced by fibrils that are ~20 nm in diameter. Both the width and stability of the craze are strongly dependent on molecular weight; increased molecular weight increases the strength of craze fibrils. The initial nucleation of a craze has also been examined (*3*). The surface microstructure of thin films of polystyrene shows sufficient heterogeneity to initiate localized strain inhomogeneities ~300 Å in diameter. As more stress is applied, cavitation ensues within these localized plastic zones to produce stable voids ~200 Å in diameter.

E. Baer and A. Hiltner are at the Department of Macromolecular Science, Case Western Reserve University, Cleveland, OH 44106. H. D. Keith is at AT&T Bell Laboratories, Murray Hill, NJ 07974.

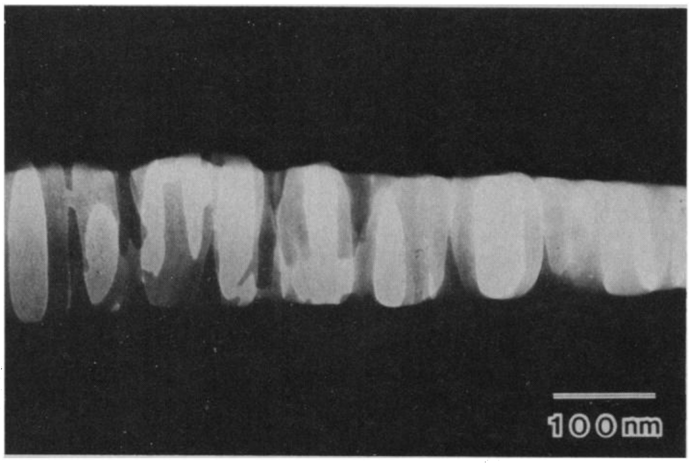

Fig. 1. Electron micrograph of a single craze in polystyrene. Thin fibrils, which are ~20 nm in diameter, are stretched across the craze boundaries. The applied strain is ~1%. Some of the fibrils have fractured; the remaining ones will break on further extension. This will lead to catastrophic crack development.

A craze front develops as more voids form along a line perpendicular to the applied stress. The kinetics of craze growth are strongly dependent on the molecular weight and the extent of cavitation that immediately precedes fibrillation.

The irreversible deformation caused by crazing can be understood with a hierarchical approach. At the molecular level, the molecular weight controls both nucleation and craze-fibril stability. At the nanolevel, the morphology and unique properties of the fibril control the process. At the microlevel, the entire craze must be considered. At the macrolevel, the bulk behavior of the crazed material can be described as a composite (*4*).

Many amorphous polymers are beneficially modified by the addition of a second toughening component. The creation of a new blend usually requires extensive research on the relations between processing, solid-state structure, and physical properties. Usually the second component is an elastomer or rubber; the impact resistance is increased while the modulus is decreased. Immiscible systems must be mixed efficiently to ensure that an optimum size distribution of domains is achieved. Numerous blends and alloys have been produced with enhanced fracture toughness and impact resistance; some are used as engineering plastics. For example, when about 10% by weight of a rubber such as chlorinated polyethylene is blended into polyvinyl chloride, large improvements in toughness and impact resistance occur (*5*). Many relatively brittle polymers, such as polystyrene, acrylonitrile-styrene copolymer, and acrylic systems, can be similarly modified with rubber to make high-performance plastics. In general, the addition of rubber stabilizes the crazing process by preventing the catastrophic formation of large cracks. Detailed hierarchical models of such modified polymers, which consider particle size distribution and interfacial characteristics, can explain these property improvements. These models are

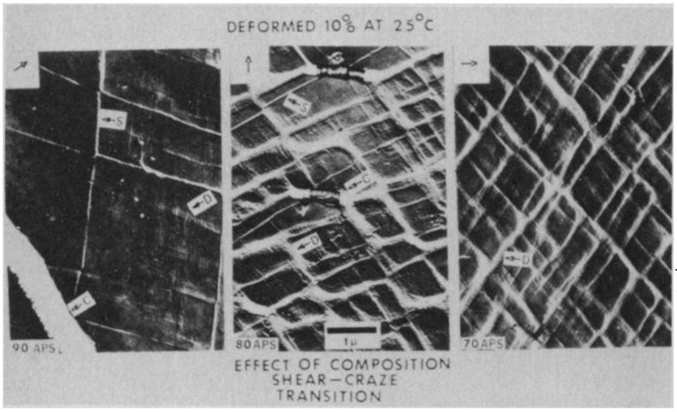

Fig. 2. Shear to craze transition to 300-nm-thick films of a blend of atactic polystyrene (APS) and PPO. The effect of composition is shown (the percentages by weight of APS are shown in the lower left corners). An arrow labeled C indicates crazing; D indicates diffuse shear banding; and S indicates sharp shear banding. The directions of the deformation (10% at 25°C) are shown in the upper left corners. As the PPO content increases, crazes grow only a short distance before they are blunted by shear bands. At the highest PPO concentration (70 APS), only diffuse shear bands appear in the blend.

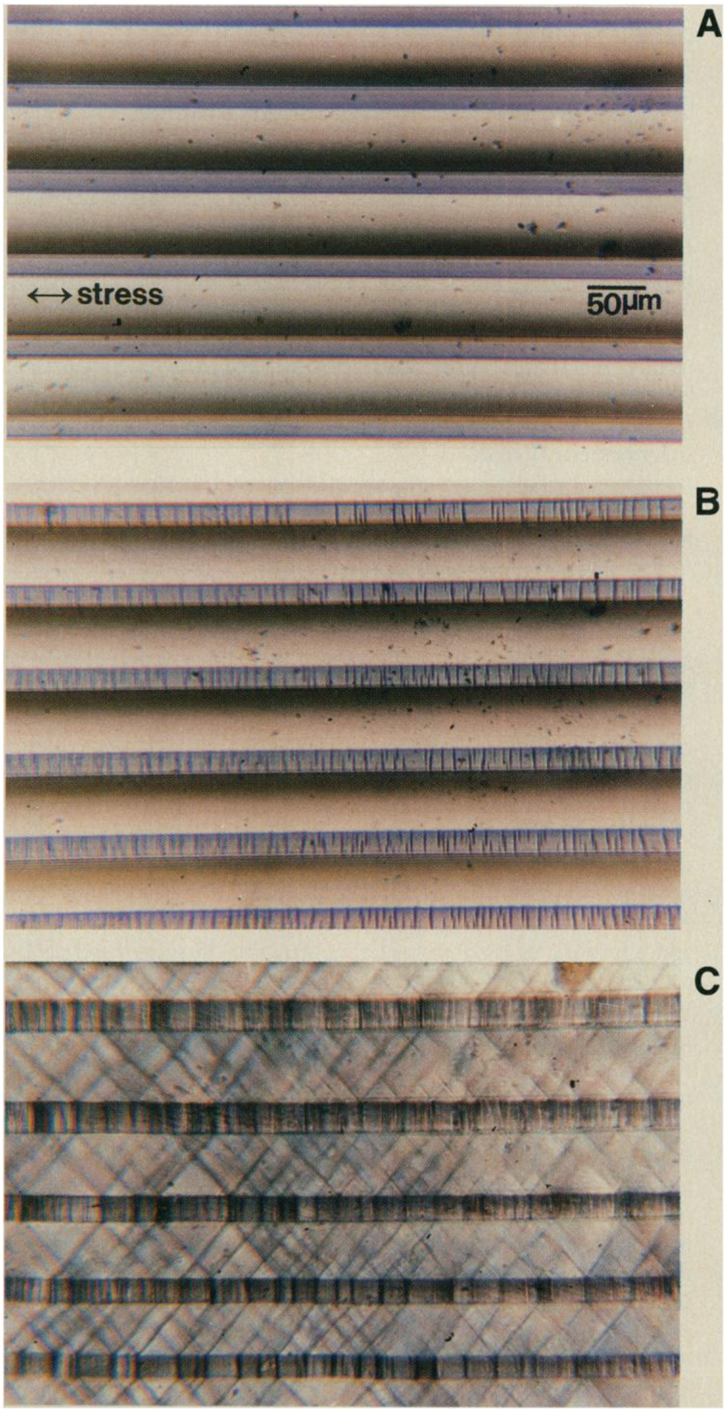

Fig. 3. Microlayer composite produced by coextrusion of polycarbonate and styrene-acrylonitrile copolymer. The three photographs (**A**, **B**, and **C**) were taken under conditions of increasing strain. The brittle layers craze and crack. Fracture is prevented by crack-tip blunting, which is caused by shear banding in the ductile layer.

sensitive to structural requirements and emphasize the interactions between scale levels. Over the past decade, a new class of high-performance blends near the 50-50 concentration range has been developed. For example, blends of polycarbonate and polyacrylonitrile-butadiene-styrene (ABS), a rubber-reinforced copolymer, are complex structures of interpenetrating phases at the nano- and microlevels. In most cases the adhesion between levels is a key variable that particularly affects the irreversible regimes of deformation and fracture.

Since amorphous polymers are some of the simplest macromolecules, there is relatively little information to be derived from the structure of the main chain. Certain important parameters that are controlled by main chain structure are the glass transition temperature and the molecular weight distribution. Unperturbed polymeric glasses of this type are relatively featureless and can be thought of as defect-ridden monolithic solids. Only when these materials are deformed irreversibly does the induced hierarchical structure emerge. Each hierarchical level usually controls a property (although a property may be dependent on many levels) and is strongly dependent on and interactive with the lower level. Reinforcing modifiers, which impart a two-phase structure to the material, are only added when the material is inadequate, or too weak, to hold the structure together. Such modifiers are usually designed to control phenomena at the nano- and microlevels.

Block copolymers are more complex than amorphous polymers. They tend to separate into microphases. The nature of the component block, which separates into phases in the solid state, can be manipulated by altering the ratio of the block length. For example, the ratio of styrene to butadiene in a diblock copolymer can be changed to control morphology. Self-organizing cylindrical, lamellar, and spherical domains are easily created. Such ordered structures give rise to distinctive properties corresponding to each of the particular morphologies (*6*).

Relatively few miscible (nonphase-separating) systems are known, the most successful of which is the blend of polystyrene and polyphenylene oxide (PPO). These two polymers are completely miscible at all concentrations. Near the 50-50 concentration range, dilational crazing failure in polystyrene, which leads to relatively brittle fracture, is entirely suppressed. A profuse shear-banding mode of irreversible deformation takes over to produce a considerably more ductile material. This is the reason for the brittle to ductile transition shown in Fig. 2. The two polymers behave in a synergistic manner to yield a tough, impact-resistant material (*7*). The irreversible deformation that controls the process changes from crazing to shear banding, because the interactions between molecular segments are modified by the intimate mixing of the two polymers. Shear processes lead to enhanced ductility and control the deformation, while the dilational crazing process is suppressed; the reasons for this are not satisfactorily understood.

Blends made by the addition of a rigid rodlike aromatic heterocyclic polymer (such as PBI, PBO, or PBT shown in Table 1) with a flexible coil-like polymer (such as nylon) are useful, because the rigid rod polymer in such blends can act as self-reinforcing molecular fiber if efficient dispersion is achieved. These blends are very stiff, even when compared to chopped fiber composites. They should have high-performance applications since they are thermally stable at relatively high temperatures, have good chemical resistance, and have a self-reinforcing character which gives high stiffnesses. The key modification occurs at the molecular level, since miscibility between a flexible and a rigid macromolecule causes the dispersivity, which in turn enhances mechanical and thermal properties.

Polymer processing has advanced rapidly in the past decade; the applications engineer has more flexibility in designing more complex polymeric structures. One novel example shown in Fig. 3 is the "microlayer" coextrusion technology (developed at the Dow Chemical Company), which permits continuous on-line processing of composite structures that can comprise as many as a few thousand layers of two or three alternating thermoplastic materials with various stacking sequences, such as ABA . . ., ABAB . . ., or ABCBABCB . . . (*8*, *9*). The compositional ratios can vary in the processing, and the layers can be a few hundred angstroms thick. Virtually all thermoplastics that can be processed into blends can be extruded in this manner. By combining two transparent polymers of different refractive indices, films can be created that have strong iridescence or that reflect ultraviolet or near-infrared radiation. Packaging films with thin multiple barrier layers can be made that do not significantly lose their original barrier properties after severe crumpling. Flaw randomization in the barrier layer causes the layer to appear continuous to a permeating gas molecule.

Table 1. Examples of polymers showing the basic chain repeat unit, the melting temperature, and the glass transition temperature. The last three polymers listed all have decomposition temperatures greater than 400°C. [Copyright 1986 by Scientific American, Inc., all rights reserved.]

Polymer	Chain unit	Melting temperature	Glass transition temperature
Polyvinylchloride	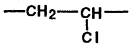 $-CH_2-CH(Cl)-$		82
Polystyrene, atactic	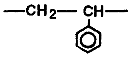		100
Polymethyl methacrylate, atactic	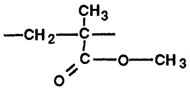 $-CH_2-C(CH_3)(C(=O)-O-CH_3)-$		105
Poly (2,2-Dimethyl phenylene oxide) (PPO)	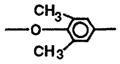		135
Polyethylene, linear	$-CH_2-CH_2-$	138	−110
Polypropylene, isotactic	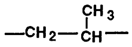 $-CH_2-CH(CH_3)-$	165	−10
Polytetrafluoroethylene	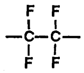 $-CF_2-CF_2-$	327	−150
Poly (p-phenylene benzobisimidazole) (PBI)	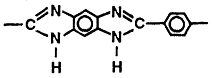		
Poly (p-phenylene benzobisoxazole) (PBO)	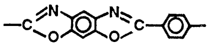		
Poly (p-phenylene benzobisthiazole) (PBT)	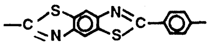		

Thick sheet can also be made with polymer layers that are alternately brittle and ductile, as shown in Fig. 3. Synergistic improvements in mechanical properties are produced. The toughness of such sheet improves monotonically with the number of layers, which illustrates architectural control at the microlevel (*9*). In Fig. 3, irreversible deformation appears initially as crazes in the layers made of the styrene-acrylonitrile copolymer. The crazes initiate shear-band formation in the polycarbonate layer so that the intense stress at the craze tip is diffused. Crack propagation is delayed because mechanical energy can now be dissipated by the ductile shear-banding layer. The extent of the interaction between the crazing and shear-banding mechanisms is controlled by the level of adhesion between the layers. The hierarchical control is entirely due to the polymer-polymer composite architecture, since no attempts were made to manipulate molecular parameters. The outcome is exceptional, since improved solid-state properties can be obtained entirely by coextrusion of two polymeric materials into a multilayered composite.

Recent advances with polymers that have relatively stiff main

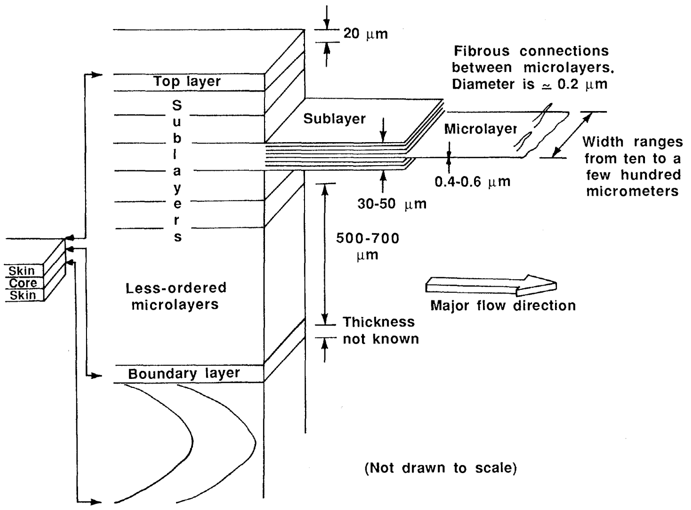

Fig. 4. Schematic illustration of a hierarchical model of an injection-molded test specimen of a liquid-crystalline polymer.

chains have been quite striking (*10*). Many of these materials are liquid-crystalline substances and are known as thermotropic polymers. Above the melting temperature, these polymers exhibit very low viscosities and flow as highly anisotropic melts. In the solid state they have high tensile strength, stiffness, and impact resistance. These properties are derived from an oriented, flow-induced hierarchical structure (*11*). In Fig. 4, the hierarchical structure of an injection-molded liquid-crystalline copolyester indicates the existence of a highly anisotropic "skin-core" structure. The high modulus of this material is derived from the flow-induced oriented skin and the toughness from the micalike layered structure.

Semicrystalline Synthetic Polymers

The occurrence of crystallinity in synthetic polymers requires a sufficiently stereoregular chemical structure to permit chain molecules in parallel orientation to pack closely in an ordered way within lattices. Structure at the nanolevel is generally determined by a pronounced tendency of these long chains to crystallize by folding back and forth within crystals of thin lamellar habit. When crystallization occurs in flowing solutions or melts, however, fine fibrous crystals may be produced that consist of highly extended chains that are oriented axially. At the microlevel, one is concerned with organization of crystalline units into spherulites or other polycrystalline structures and with modes of elastic or plastic deformation. Properties on the macrolevel must then be interpreted in terms of the behavior of assemblies of these various components at both nano- and microlevels. The development of molecular order is usually limited severely by kinetic restraints. Even after prolonged crystallization from the melt, there always remains an appreciable volume fraction of a disordered phase which is generally called "amorphous," although it may not always be so structureless as the term suggests. [For a general background see (*12*).]

Lamellar polymer crystals are on the order of 10 nm thick. Straight segments of molecules (stems) are oriented in directions essentially normal to lamellar planes; each molecule traverses a crystal many times between folds at upper and lower surfaces. Growth occurs by addition onto narrow lateral faces. Crystals of fairly regular geometrical outline, in which fairly regular folding occurs predominantly with reentry at adjacent lattice sites, are usually formed by slow growth at temperatures close to melting points (Fig. 5). More rapid crystallization at lower temperatures introduces considerable disorder both in terms of regularity of folding and molecular packing at fold surfaces. "Loose loops" and nonadjacent reentry then become common at fold surfaces and, in highly crystalline polymers, the amorphous phase occurs mostly as disordered layers at these surfaces. Despite such disorder, a clearly lamellar morphology is still seen in electron microscopic studies of polymers that are solidified from quiescent melts under conditions of fast crystallization or large melt viscosity. An important consequence of crystallization under such conditions is formation of "tie molecules," which are short chain lengths that bridge neighboring crystals, and of more substantial intercrystalline links in the form of short fibers on the order of 10 nm in diameter (*13*) as shown in Fig. 6. Together, these play a major role in mechanical properties by restricting interlamellar slippage or cleavage and by initiating substantial morphological changes during plastic deformation.

If structure is to be understood at the nanolevel, then it must be explained why and how long chains, which are initially in disordered random coil conformations, fold at crystal growth fronts. Two important aspects must be considered. First, a high incidence of relatively tight folding is required because, without tight folding, chains would emerge from the surface of a lamellar crystal into an amorphous region of substantially smaller density and would cause prohibitive congestion on the disordered side of the phase boundary (*14*). Second, observed growth kinetics suggest that the rate-determining step in crystallization is nucleation of new layers on growth fronts. A theoretical analysis of such nucleation, initiated by Lauritzen and Hoffman (*15*), has shown that the growth rate of a chain-folded lamellar crystal should exhibit a fairly sharp maximum when lamellar thickness exceeds only slightly (by 1 to 2 nm) the minimum thickness necessary for thermodynamic stability. This result is in excellent agreement with experimental observation both with regard to lamellar thickness and to its inverse variation with the supercooling at which crystallization occurs. An extensive kinetic theory of polymer crystallization has now been developed that accounts well for many subtleties of observed behavior. [For a discussion of recent developments, see (*16*).] An important consideration has nevertheless been bypassed until recently. The unit of addition during crystallization has been considered to be, in effect, a complete molecular stem that reaches across an entire growth face. Sadler and Gilmer (*17*) have now addressed the finer details of molecular attachment from the standpoint of roughening transitions at crystal surfaces.

Growth of fibrous crystals from sheared solutions or melts,

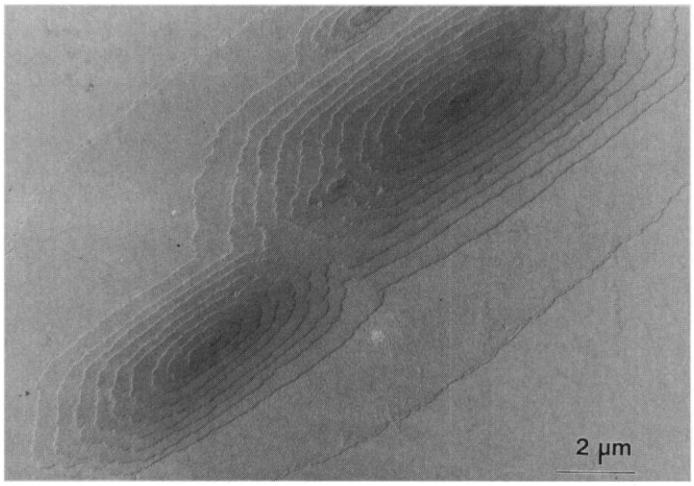

Fig. 5. Electron micrograph of a lamellar crystal of poly(ε-caprolactone) showing development of new layers at growth spirals around screw dislocations.

especially when elongational flow (*18*) is involved, is a consequence of the considerable distortion of coils into elongated conformations before and during solidification. Molecules of higher molecular weight are particularly susceptible to such effects, and shorter chains often crystallize subsequently into folded conformations on lateral surfaces of the fibers to form structures called "shish kebabs" (*19*).

Primary nucleation occurs at specific sites in quiescent polymer melts, often at dust or catalyst particles, and initiates the growth of spherulites. These are globular aggregates that consist of many closely packed lathlike lamellar crystals (≈ 0.1 to 5 μm wide) that fan outward from a center. Frequent branching at screw dislocations ensures more or less uniformly space-filling fibrillar texture. Outward growth continues until it is halted by contact with neighboring spherulites (*20*). The spherulites, which are the prominent structural units on the microlevel, are usually on the order of 10 μm in diameter. The resulting structure is reminiscent of a polycrystalline metal (Fig. 7), but the "grains" (the spherulites) are polycrystalline and exhibit little preferred orientation overall, although a single fast-growing crystal axis is usually highly oriented along radii.

Texture within spherulites is strongly dependent on crystallization temperature. A major factor is the segregation of shorter chains, and of stereoirregular chains if present, at crystal growth fronts. Segregated species become redistributed by localized diffusion on a scale governed by a length parameter that is determined by the diffusive mobility of the chains and the growth rate of the crystals (*20*). At higher crystallization temperatures these species accumulate between stacks or clusters of lamellae, and to some extent between individual lamellae as well, where they may subsequently crystallize or remain as part of the amorphous phase. As the crystallization temperature is lowered, the scale of redistribution becomes smaller and the texture becomes correspondingly finer, until a stage is reached such that there is little segregation of shorter chains. Crystallization then involves segmental motion rather than diffusion of entire chains. Reduction of the crystallization temperature also enhances considerably the connectedness of neighboring crystals by tie molecules and intercrystalline links. Polymers crystallized comparatively slowly at higher temperatures tend to be brittle; those crystallized more rapidly at lower temperatures become ductile and tough.

Small stresses applied above the glass transition temperature of the amorphous phase cause strains that are confined almost entirely to this phase, but details of deformation under larger stresses depend markedly on the local orientation of lamellae with respect to the principal stress axes. Lamellae under tension within their own planes respond almost immediately by cracking, the cracks being copiously bridged by fine microfibrils that are formed when extended chains are pulled out of their folded conformations (*21*). In obliquely oriented stacks of lamellae there is initially some interlamellar slippage and some shear within the crystals (*22*). However, local strains that are greater than about 50% cause a progressive disruption of the crystalline order that was produced by tie molecules and intercrystalline links, which in fact function as stress concentrators. Spherulites in specimens that are deformed by unidirectional tension readily form fibrils along radii parallel to the stress axis but yield more gently along transverse directions. At large elongations, a highly oriented structure is formed that consists of microfibrils about 10 to 20 nm in diameter (*21*). The polymer then exhibits considerable strength in the direction of orientation but is weak when loaded transversely. Yielding is more homogeneous when spherulites are deformed by uniaxial compression. Changes in hierarchical structure, which involve breakup, reorientation, and recrystallization of lamellae (Fig. 8), cause an enhancement in toughness (*23*).

The influence of structure at different hierarchical levels upon macroscopic mechanical properties of polymers can be best illustrated by comparing observed behavior with theoretical limits imposed at a fundamental level by interatomic forces (*24*). Tensile moduli of crystals stressed along chain directions can be estimated from interatomic force constants to be about 10 GPa when strains involve rotation around bonds (with helical conformations) and about 100 GPa when there is an opening of bond angles (with planar zigzag conformations). Moduli of about 120 GPa have been observed in specially prepared polyethylene fibers that have high degrees of orientation. Moduli of unoriented polymers are small by comparison because of the compliance of amorphous phases (~ 0.1 GPa when these are rubbery, as in polyethylene, and ~ 2 GPa when they are glassy, as in nylon). It has been estimated that a force of about 5 nN is required to rupture a covalent bond. On this basis the

Fig. 6. Electron micrograph showing intercrystalline links (indicated by arrowheads) between lamellae in a sample of polyethylene.

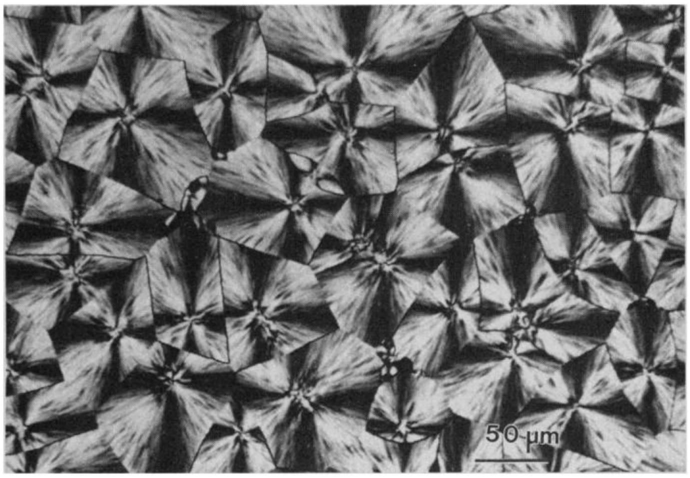

Fig. 7. Polarizing optical micrograph of a typical spherulitic structure in a polymer film crystallized from the melt.

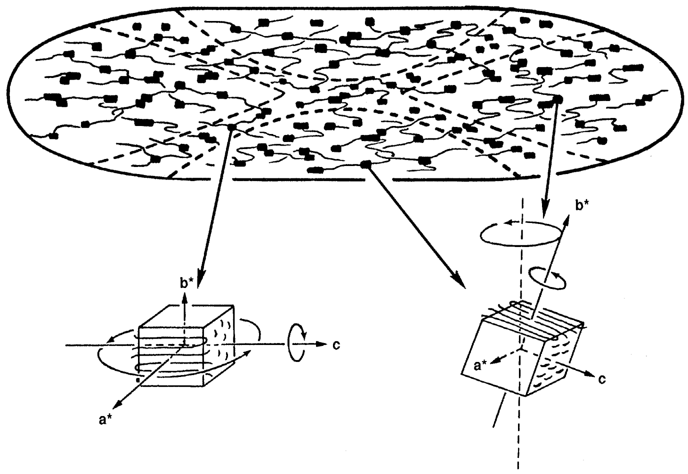

Fig. 8. Hierarchical model of flattened spherulite showing the breakup of lamellae into oriented crystalline blocks.

theoretical tensile strength of a highly oriented polymer should be ~20 GPa. Measured tensile strengths are at least one, and commonly two, orders of magnitude smaller, because structural imperfections cause sequential rather than simultaneous breakage of bonds during failure. Theoretical strengths in directions transverse to chain axes in crystals are considerably smaller; cooperative rupture of van der Waals bonds should require a stress on the order of 100 MPa; similar rupture of densely hydrogen-bonded structures, as in nylons, should require about 500 MPa.

Typical behavior in the drawing of unoriented semicrystalline polymers is readily explained in terms of these estimates. Yielding occurs at a strain typically of 1 to 10%; significant disruption of chain-folded crystals begins. Since yield stress is related to the force required to pull neighboring chains apart in real crystals, observed values are in the range of 10 to 30 MPa when bonding is exclusively of the van der Waals type, and about 60 MPa when polar interactions are also involved. Chain folding (nanolevel structure) underlies the observed insensitivity of these values to changes in molecular weight, and also the fact that large elongations and high degrees of orientation can be obtained so readily. A strong tendency for plastic deformation to begin in highly localized regions is related to spherulitic structure on the microscale. Radial orientation of lamellae always provides circumstances favorable for initiation of localized catastrophic disruption of lamellae; yielding then propagates from these regions becuase of the resulting stress concentration.

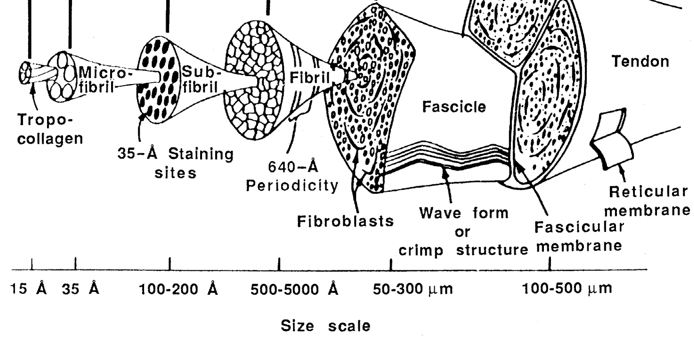

Fig. 9. Hierarchical model of tendon showing discrete levels of organization. Abbreviations: DSC, differential scanning calorimetry; EM, electron microscopy; SEM, scanning electron microscopy; OM, optical microscopy.

An elegant example of how unusual properties may be achieved through control of hierarchical structure is provided by "hard-elastic" polymers, which are somewhat highly crystalline but behave elastically up to surprisingly large uniaxial strains (50 to 100%) (*25*). These have networks of oriented fibrous crystals that are bridged by transverse lamellae. Under uniaxial stress the structure opens up like a concertina. Recovery upon relaxation of the stress is almost complete.

Soft Connective Tissue

Soft connective tissues, designed to serve specific functions in man and animals, are among the most advanced macromolecular composites known. Such tissues possess a hierarchical architecture made from a small number of components. In general, these multicomposite structures consist of collagen fibrils embedded in a gel-like matrix. Two examples emphasize their role in nature. Tendon operates mainly in uniaxial tension and serves as the primary connecting linkage between muscle and bone; intervertebral disk serves in compression and shear as a pad between rigid bone structures.

The collagen fibril is an oriented composite structure (Fig. 9) (*26*). The chains, which are uniformly 290 nm long, form a triple helical structure called tropocollagen. An essential feature for the formation of the triple helix is that every third unit along the chain is glycine. The arrangement of polar and hydrophobic amino acids in clusters along the molecule is responsible for the assembly into fibrillar structures. It is generally believed that four or five tropocollagen molecules aggregate at the nanolevel to form a fibrous entity termed the microfibril, which is 3.6 nm in diameter. The strongest polar and hydrophobic interactions occur when neighboring molecules are shifted by 67 nm, which is called the "stagger." This stagger, combined with a gap between the ends of consecutive molecules, is responsible for the characteristic periodicity that can be observed by electron microscopy and x-ray diffraction methods. It follows that such microfibrils have both polar and nonpolar regions, which are readily accessible to specific inter- and intrafibrillar interactions. The microfibrils are thought to pack in a tetragonal lattice to form subfibrils about 30 nm in diameter. These subfibrils would then assemble into the collagen fibril. This step in the assembly also appears to be controlled at least in part by the primary structure of collagen, but it is not clear how the diameter of the fibril, which varies from 50 to 500 nm (depending on tissue and animal maturity), is determined.

Fibrils are surrounded by the extrafibrillar matrix and are oriented in a hierarchical architecture to form specific soft tissues. The fact that collagen can be organized in different macromolecular structures indicates that this process cannot be regulated by the amino acid sequence alone. Other mechanisms, including interaction with noncollagenous components, must play a role. The primary macromolecular component of the matrix is a highly branched aggregate of subunits. The proteoglycan subunits consist of a core protein with numerous pendant mucopolysaccharide molecules. The subunits in turn are attached as branches to high molecular weight hyaluronic acid. When swollen with water, this ultrahigh molecular weight proteoglycan aggregate forms an extremely efficient network structure which connects and maintains the hierarchical architecture of collagen fibrils. The properties of this matrix material are strongly dependent on and regulated by the large quantities of bound and free water.

Three interstitial collagen types have been identified. Types I, II, and III collagen differ in their primary sequence of amino acids; these differences would be expected to influence the nature of aggregation. Nevertheless, all appear to form fibrils with the same molecular stagger, which reflects the close similarity in sequence of polar amino acids. In general, type I collagen is present in tissues as parallel bundles of thick fibers; types II and II are more likely to form fine network structures (*27*). There is evidence that when present in the same tissue, the different collagen types form separate architectures that serve specific mechanical functions (*28*).

Tendon is a uniaxial structure with parallel assembly of type I collagen fibrils to form larger fibers. The fibers have a regular wavy configuration on the microlevel (Fig. 10A) (*29, 30*). When viewed in the polarizing optical microscope, the wavy fibers produce a characteristic banding pattern of bright and dark extinctions. The wave form, which is a planar zigzag rather than a helix (*29*), has been confirmed by other methods (*31*). Nevertheless, the origin of the waviness has not been explained. Arrays of crimped fibers, which are much like ribbons, are organized into fascicles that are roughly triangular in cross section and have a diameter of 150 to 300 μm (*32*). These fascicles constitute the basic tendon unit at the macroscale.

The initial response of the tendon to stress is the gradual straightening of the wavy fibers. This corresponds in the stress-strain relation to a region of small but gradually increasing slope. Some models of the mechanical behavior consider only the elastic behavior at low strains (*33–35*). Models for the viscoelastic behavior are generally phenomenological and use combinations of nonlinear springs and dashpots (*35, 36*). Although these models accurately reproduce the mechanical behavior of tendon, they do not include actual tendon morphology and therefore have little structural significance. The experimental data have been fitted accurately by models that are based on the actual morphology and that treat the tendon as a composite of wavy elastic fibers in a viscoelastic matrix (*33*). This approach also reproduces the effects of maturation and aging on the mechanical properties of tendon by incorporating changes observed in the shape of the wave form. Surprisingly, the modulus of the extended collagen fibers does not change during aging (*37*).

Although the elastic properties of tendon in the physiological range are determined by the size level of the wave form, the damage processes which determine the ultimate strength of tendon involve the entire hierarchical structure. The fibril size distribution of tendon in rat tail changes considerably during maturation and aging (*38*). For newborn rats, the fibrils are uniformly about 30 nm in diameter. During maturation and aging the size increases to a maximum of about 450 nm. The distribution in the mature tendon is very broad; the small fibrils fill the voids between larger ones to produce a packing arrangement with a very high volume fraction of fibrils. Proteoglycan makes up less than 1% of the dry weight of the tendon. When hydrated, it forms a continuous matrix between the fibrils and provides the adhesion that gives the tendon lateral integrity. Dissociation of the fibril into microfibrils and subfibrils, and slippage of collagen molecules within these entities, are the primary damage mechanisms when rat tail tendon is deformed beyond the elastic limit (*37*). The fibril becomes more resistant to these damage processes with aging.

The intervertebral disk is composed of two anatomical structures, the annulus fibrosis, a lamellar structure of collagen fibers, and the nucleus pulposis, a gelatinous hydrophilic material. The annulus fibrosis is composed of concentric, cylindrical lamellae about 150 μm in diameter. Within the lamellae, the collagen fibers are parallel to one another and assume a planar wave-form configuration (Fig. 10B) which is oriented in and out of the plane of the lamellae. The overall orientation of fibers alternates in succeeding lamellae from +30° to −30° to the transverse anatomic direction (*39*). The ends of the fibers are incorporated into the cartilaginous end plates, thus securely anchoring the disk to the vertebrae (*40*). The lamellae are densely layered at the periphery of the disk but gradually become thinner and more highly separated toward the interior. A poorly defined transition zone separates the annulus fibrosis from the nucleus pulposis, which is an oval gelatinous structure that occupies the center of the disk. The intervertebral disk is composed of type I and II collagen. At the periphery of the annulus fibrosis more than 95% of the collagen is type I. This percentage decreases along an approximately linear gradient to a level of less than 5% in the nucleus pulposis (*41*). It has been suggested that type I collagen fibers form the lamellae while type II collagen exists as a network in the nucleus pulposis and may also be present in the interlamellar regions.

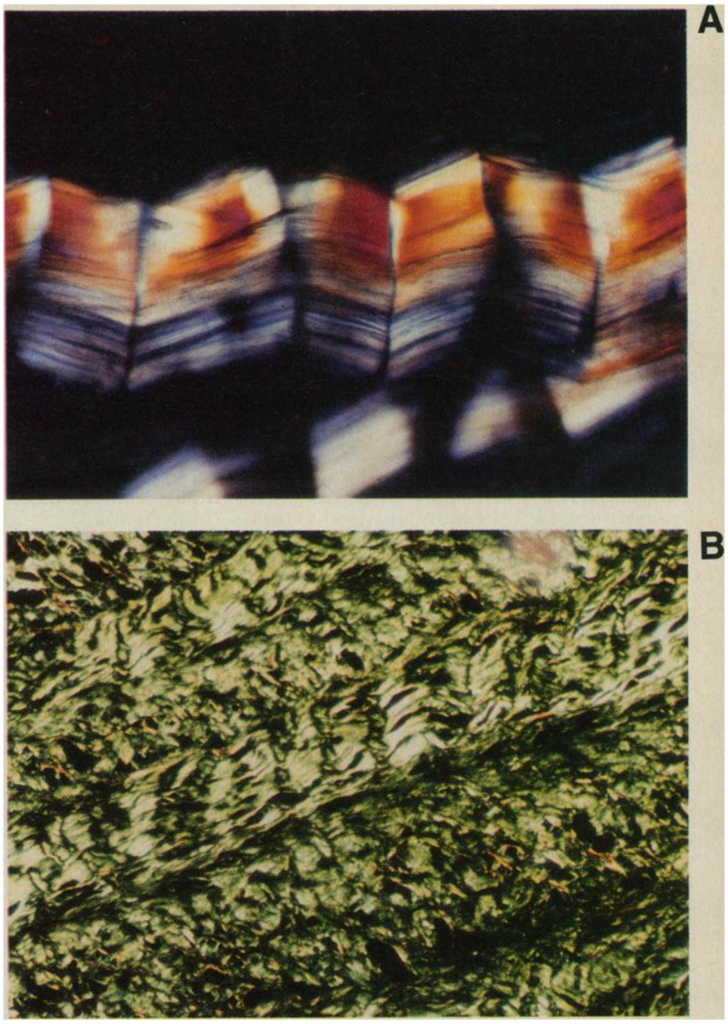

Fig. 10. Optical micrographs of (**A**) rat-tail tendon fascicle, which shows the planar-crimp structure and uniaxially oriented textures, and (**B**) intervertebral disk, which shows a section of the annulus fibrosis. The annulus is composed of concentric, cylindrical lamellae. The collagen fibers assume a planar wave form.

The mechanical function of the nucleus is to maintain the height of the disk under compressive loading and to transmit stress to the lamellae of the annulus (*42*). The disk bulges under compressive loading, which indicates that axial loads are transmitted into tensile hoop stresses in the lamellae of the annulus (*43*). Thus compressive forces are transformed into tensile stresses on the collagen fibers of the lamellae. The response of the fibers is to straighten the wave form (*44*) and to rotate somewhat with respect to the axial orientation (*45*). The collagen fibers perform more efficiently in tension than in compression. The disk is designed to use this strength so that the primary load-bearing elements, the collagen fibers of the lamellae, can respond in tension, although the structure must function in compression.

The analysis of complex behavior in natural and synthetic polymeric systems in terms of hierarchies is an approach that interrelates our understanding of structure at various scales. Such an approach may prove invaluable in the design of new advanced polymers. Structural hierarchy is more than a covenient vehicle for description and analysis. Important and difficult questions that remain to be addressed include the physical and chemical factors that give rise to relatively discrete levels of structure and the relations that govern their scaling.

REFERENCES AND NOTES

1. A. L. Bement, Jr., American Society for Metals and the Metallurgical Society Joint Distinguished Lecture in Materials and Society, "The greening of materials science and engineering," Materials Week—1986, Orlando, 7 October 1986.
2. E. Baer, *Sci. Am.* **255**, 179 (October 1986).
3. S. Wellinghoff and E. Baer, *J. Macromol. Sci. Phys.* **11** (no. 3), 367 (1975).
4. A. Moreno and E. Baer, in *Structure-Property Relationships of Polymeric Solids*, A. Hiltner, Ed. (Plenum, New York, 1983), pp. 1–24.
5. A. Siegmann and A. Hiltner, *Polym. Eng. Sci.* **24**, 369 (1984); A. Siegmann, L. K. English, E. Baer, A. Hiltner, *ibid.*, p. 877.
6. J. M. G. Cowie, in *Developments in Block Copolymers-1*, I. Goodman, Ed. (Applied Science, London, 1982), pp. 1–37.
7. S. Wellinghoff and E. Baer, *J. Appl. Polym. Sci.* **22**, 2025 (1978).
8. W. J. Schrenk and T. Alfrey, Jr., in *Polymer Blends*, D. R. Paul and S. Newman, Eds. (Academic Press, New York, 1978), vol. 2, pp. 129–165.
9. B. L. Gregory, A. Siegmann, J. Im, A. Hiltner, E. Baer, *J. Mater. Sci.*, in press.
10. T. Chung, *Polym. Eng. Sci.* **26**, 901 (1986).
11. T. Weng, A. Hiltner, E. Baer, *J. Mater. Sci.* **21**, 744 (1986); L. C. Sawyer and M. Jaffe, *ibid.*, p. 1897.
12. F. Khoury and E. Passaglia, in *Treatise in Solid State Chemistry*, N. B. Hannay, Ed. (Plenum, New York, 1976), vol. 3, chap. 6; D. C. Bassett, *Principles of Polymer Morphology* (Cambridge Univ. Press, Cambridge, 1981).
13. H. D. Keith, F. J. Padden, Jr., R. G. Vadimsky, *J. Appl. Phys.* **42**, 4585 (1971).
14. F. C. Frank, in *Growth and Perfection of Crystals*, R. H. Doremus and D. Turnbull, Eds. (Wiley, New York, 1958), pp. 3–9; *Discuss. Faraday Soc.* **68**, 7 (1979).
15. J. I. Lauritzen, Jr., and J. D. Hoffman, *J. Res. Natl. Bur. Stand. Sect. A* **64**, 73 (1960).
16. J. D. Hoffman, G. T. Davis, J. I. Lauritzen, Jr., in *Treatise in Solid State Chemistry*, N. B. Hannay, Ed. (Plenum, New York, 1976), vol. 3, chap. 7; J. D. Hoffman, C. M. Guttman, E. A. DiMarzio, *Discuss. Faraday Soc.* **68**, 177 (1979); J. D. Hoffman, *Polymer* **24**, 3 (1983).
17. D. M. Sadler, *Polymer* **24**, 1401 (1983); ______ and G. H. Gilmer, *ibid.* **25**, 1446 (1984); *Phys. Rev. Lett.* **56**, 2708 (1986).
18. C. J. S. Petrie, *Elongational Flows* (Pittman, White Plains, NY, 1979).
19. A. J. Pennings, J. M. van der Mark, A. M. Kiel, *Kolloid Z. Z. Polym.* **237**, 336 (1970).
20. H. D. Keith and F. J. Padden, Jr., *Polymer* **27**, 1463 (1986).
21. A. Peterlin, in *Structure and Properties of Oriented Polymers*, I. M. Ward, Ed. (Wiley, New York, 1975), pp. 36–56.
22. C. A. Garber and E. S. Clark, *J. Macromol. Sci. Phys.* **4**, 499 (1970).
23. S. J. Pan, H. R. Brown, A. Hiltner, E. Baer, *Polym. Eng. Sci.* **26**, 997 (1986).
24. L. Holliday, in *Structure and Properties of Oriented Polymers*, I. M. Ward, Ed. (Wiley, New York, 1975), pp. 242–263.
25. S. L. Cannon, G. B. McKenna, W. O. Statton, *J. Polym. Sci. Macromol. Rev.* **11**, 209 (1976).
26. E. Baer, L. J. Gathercole, A. Keller, in *Structures of Fibrous Proteins*, E. D. T. Atkins and A. Keller, Eds. (Butterworth, London, 1975), pp. 189–195.
27. K. Kuhn and R. W. Glanville, in *Biology of Collagen*, A. Viidik and J. Vuust, Eds. (Academic Press, New York, 1980), pp. 1–14.
28. A. Hiltner, J. J. Cassidy, E. Baer, *Annu. Rev. Mater. Sci.* **15**, 455 (1985).
29. J. Diamant, A. Keller, E. Baer, M. Litt, R. G. C. Arridge, *Proc. R. Soc. London Ser. B* **180**, 293 (1972).
30. B. J. Rigby, N. Hirai, J. D. Spikes, H. Eyring, *J. Gen. Physiol.* **43**, 265 (1959); A. Viidik and R. Ekholm, *Z. Anat. Entwicklungsgesch.* **127**, 154 (1968).
31. L. J. Gathercole, A. Keller, J. S. Shah, *J. Microsc. (Oxford)* **102**, 95 (1974); J. Dlugosz, L. J. Gathercole, A. Keller, *Micron* **9**, 71 (1978); L. J. Gathercole and A. Keller, *Biochim. Biophys. Acta* **535**, 253 (1978).
32. H. Niven, E. Baer, A. Hiltner, *Collagen Relat. Res.* **2**, 131 (1982).
33. J. Kastelic, E. Baer, I. Palley, *J. Biomech.* **13**, 887 (1980).
34. B. D. Coleman and H. Markovitz, *J. Polym. Sci. Polym. Phys. Ed.* **12**, 2195 (1974).
35. A. Viidik, *J. Biomech.* **1**, 3 (1968).
36. ______, *Int. Rev. Connect. Tissue Res.* **6**, 127 (1973); N. Frisen, M. Magi, L. Sonnerup, A. Viidik, *J. Biomech.* **2**, 13 (1969); V. H. Frankel and A. H. Burstein, in *Orthopaedic Biomechanics* (Lea & Fibiger, Philadelphia, 1970), p. 188.
37. J. Kastelic and E. Baer, *The Mechanical Properties of Biological Materials*, J. F. V. Vincent and J. D. Currey, Eds. (Society for Experimental Biology, London, 1980), pp. 397–455.
38. S. Torp, E. Baer, B. Friedman, in *Structures of Fibrous Proteins*, E. D. T. Atkins and A. Keller, Eds. (Butterworth, London, 1975), pp. 223–250.
39. D. S. Hickey and D. W. L. Hukins, *J. Anat.* **131** (no. 3), 81 (1980).
40. H. Inoue and T. Takeda, *Acta Orthop. Scand.* **46**, 949 (1975).
41. P. Adams, D. R. Eyre, H. Muir, *Rheumatol. Rehabil.* **16**, 22 (1977); C. Berthet-Colominas, A. Miller, D. Herbage, M. Ronziere, D. Tocchetti, *Biochim. Biophys. Acta* **706**, 50 (1982); D. R. Eyre and H. Muir, *Biochem. J.* **157**, 267 (1976); *FEBS Lett.* **42** (no. 2), 192 (1974).
42. A. Nachemson, *Acta. Orthop. Scand.* **33**, 183 (1963).
43. K. L. Markolf and J. M. Morris, *J. Bone Jt. Surg. Am. Vol.* **56** (no. 4), 675 (1974).
44. J. J. Cassidy, A. Hiltner, E. Baer, unpublished results.
45. J. A. Klein and D. W. L. Hukins, *Biochim. Biophys. Acta* **717**, 61 (1982); *ibid.*, p. 98.